PHILOSOPHICAL TRANSACTIONS OF THE ROYAL SOCIETY B

rstb.royalsocietypublishing.org

Research

Cite this article: Korotchenko S, Cingolani LA, Kuznetsova T, Bologna LL, Chiappalone M, Dityatev A. 2014 Modulation of network activity and induction of homeostatic synaptic plasticity by enzymatic removal of heparan sulfates. *Phil. Trans. R. Soc. B* **369**: 20140134. http://dx.doi.org/10.1098/rstb.2014.0134

One contribution of 23 to a Theme Issue 'Brain circuitry outside the synaptic cleft'.

Subject Areas:
neuroscience, physiology, cellular biology

Keywords:
heparan sulfate proteoglycans, AMPA receptor, neural network, burst, seizure, synaptic upscaling

Author for correspondence:
Alexander Dityatev
e-mail: alexander.dityatev@dzne.de

†These authors contributed equally to this study.

Electronic supplementary material is available at http://dx.doi.org/10.1098/rstb.2014.0134 or via http://rstb.royalsocietypublishing.org.

Royal Society Publishing

Modulation of network activity and induction of homeostatic synaptic plasticity by enzymatic removal of heparan sulfates

Svetlana Korotchenko[1,2,†], Lorenzo A. Cingolani[1,†], Tatiana Kuznetsova[1,†], Luca Leonardo Bologna[3,4,5], Michela Chiappalone[1] and Alexander Dityatev[1,2,6]

[1]Department of Neuroscience and Brain Technologies, Istituto Italiano di Tecnologia, via Morego 30, 16163 Genoa, Italy
[2]Laboratory for Brain ECM Research, State University of Nizhny Novgorod, 603950 Nizhny Novgorod, Russia
[3]INSERM, U968, Paris 75012, France
[4]Sorbonne Universités, UPMC Univ Paris 06, UMR_S 968, Institut de la Vision, Paris 75012, France
[5]CNRS, UMR_7210, Paris 75012, France
[6]Molecular Neuroplasticity Group, German Center for Neurodegenerative Diseases (DZNE), 39120 Magdeburg, Germany

Heparan sulfates (HSs) are complex and highly active molecules that are required for synaptogenesis and long-term potentiation. A deficit in HSs leads to autistic phenotype in mice. Here, we investigated the long-term effect of heparinase I, which digests highly sulfated HSs, on the spontaneous bioelectrical activity of neuronal networks in developing primary hippocampal cultures. We found that chronic heparinase treatment led to a significant reduction of the mean firing rate of neurons, particularly during the period of maximal neuronal activity. Furthermore, firing pattern in heparinase-treated cultures often appeared as epileptiform bursts, with long periods of inactivity between them. These changes in network activity were accompanied by an increase in the frequency and amplitude of miniature postsynaptic excitatory currents, which could be described by a linear up-scaling of current amplitudes. Biochemically, we observed an upregulation in the expression of the glutamate receptor subunit GluA1, but not GluA2, and a strong increase in autophosphorylation of α and β Ca^{2+}/calmodulin-dependent protein kinase II (CaMKII), without changes in the levels of kinase expression. These data suggest that a deficit in HSs triggers homeostatic synaptic plasticity and drastically affects functional maturation of neural network.

1. Introduction

Heparan sulfates (HSs) are unbranched sulfated polysaccharides composed of glucuronic acid and *N*-acetylglucosamine. During their biosynthesis in the Golgi apparatus, these glycosaminoglycans are highly modified by sulfation and C5 epimerization of glucuronic acid, leading to heterogeneity in HS structures. Specific combinations of glycosaminoglycan-modifying enzymes generate specific functional microdomains in the glycosaminoglycan chains, which bind selectively with various growth factors, morphogens, axon guidance molecules and extracellular matrix (ECM) proteins [1].

HSs are covalently attached to proteoglycans (HSPGs), among which are ECM molecules perlecan, agrin, collagen XVIII and cell surface molecules such as glypicans and syndecans. The latter can be shed and incorporated into the ECM through interactions with fibronectin, laminins, endostatin, thrombospondins and collagens [2]. During neural development, HSPGs modulate signalling through key regulatory secreted proteins such as bone morphogenetic protein, fibroblast growth factor (FGF) and sonic hedgehog protein by acting on their receptor activation and signal spreading [3]. Interaction between HSPGs and the polysialylated form of the neural cell adhesion molecule (NCAM) was originally found to stimulate NCAM-dependent synaptogenesis in an FGF and

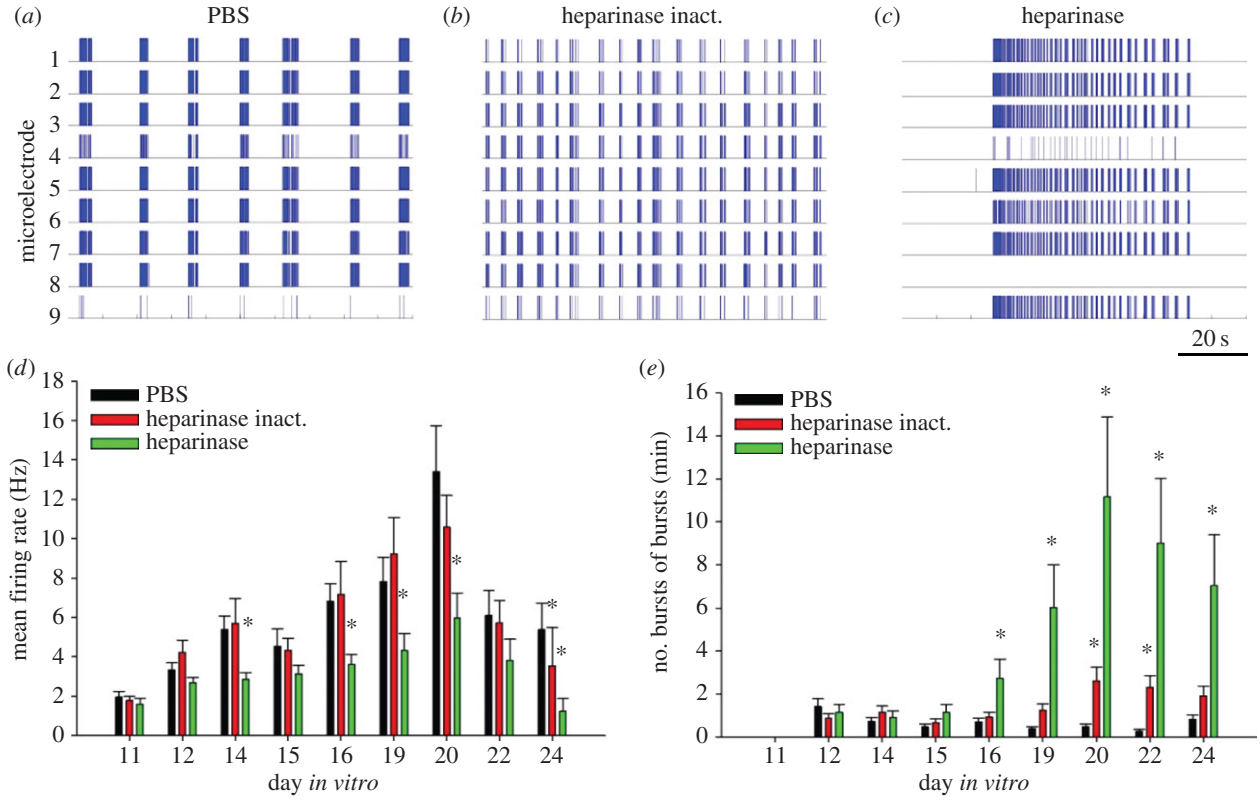

Figure 1. Heparinase treatment induces epileptiform spiking activity. Raster plots of spontaneous spiking activity in primary hippocampal cultures at DIV 20, treated with PBS (*a*), heat-inactivated heparinase (*b*) or active heparinase (*c*). Scale bar is 20 s, valid for (*a*–*c*). Each stick of represented raster plots shows a spike recorded from one of nine electrodes of the microelectrode array. A high synchronization of activity recorded in most electrodes is obvious. The duration of demonstrated raster plots is 100 s. Neurons treated by heparinase show abnormally long (up to 70 s) epileptiform bursts of bursts, whereas cultures from control groups show shorter regular bursting episodes. A difference in bursting pattern in (*a*) and (*b*) reflects physiological variability, common for both control conditions. Developmental changes of mean firing rate (*d*) and mean frequency of bursts of bursts (*e*) in treated cultures. Both parameters of neuronal network activity reach the maximum at DIV 20. Increase of epileptiform activity in heparinase-treated cultures parallels the fall in overall mean firing rate relative to control groups. Data are presented as the mean $\pm$ s.e.m., $n = 15-17$. Statistical analysis was performed using a two-way analysis of variance (ANOVA), SNK was used as a post hoc ANOVA test. The difference between groups was considered significant if $^*p < 0.05$. (Online version in colour.)

N-methyl-D-aspartate (NMDA) receptor-dependent manner [4]. A more recent study identified glypicans 4 and 6 as astrocyte-secreted signals sufficient to induce functional excitatory synapses by increasing the surface level and clustering, but not overall cellular protein level, of the GluA1 subunit of the AMPA (α-amino-3-hydroxy-5-methyl-4-isoxazole propionic acid) glutamate receptors (AMPARs) [5]. Acute enzymatic treatment of hippocampal slices with heparinases results in a reduction of long-term potentiation in CA3–CA1 synapses and prevents the increase in the density of perforated synapses normally associated with induction of long-term potentiation [4,6]. Conditional inactivation of *Ext1*, the gene encoding an enzyme essential for HS synthesis, recapitulates a number of autistic symptoms, including impairments in social interaction, expression of stereotyped, repetitive behaviour and impairments in ultrasonic vocalization [7].

Here, we aimed at investigating the effects of HS removal at the network level and at dissecting the underlying synaptic and molecular mechanisms. Unlike previous studies of synaptic plasticity [4,6], which used a mixture of heparinases, we treated cultured dissociated hippocampal neurons with heparinase I, which preferentially cleaves highly sulfated heparan sulfates (HSHSs), thus allowing us to assess the function of specific HS moieties. Our results demonstrate that a deficit of this type of HSs leads to appearance of long-lasting neuronal discharges separated by long intervals of neuronal silence, so the mean neuronal firing rate is reduced. At the synaptic level, these changes were accompanied by homeostatic plasticity in the form of synaptic up-scaling [8], i.e. excitatory synapses on pyramidal cells were equally 'scaled up' due to the increase in postsynaptic AMPA receptor expression, as detected by analysis of miniature excitatory postsynaptic current (mEPSC) amplitude distribution.

2. Results

(a) Abnormal network activity after heparinase treatment

Chronic treatment of hippocampal cultures with heparinase I (0.5 U ml^{-1}) was performed starting from 11th day *in vitro* (DIV) to avoid potential effects of enzyme on early neuronal differentiation. The treatment did not affect cellular composition of cultures containing both MAP2-immunopositive neurons and GFAP-immunopositive astrocytes (electronic supplementary material, figure S1). In microelectrode recordings, heparinase treatment resulted in the appearance of long-lasting epileptiform discharges (figure 1*c*). These spike bursts lasted up to 70 s at DIV 17–20 and were separated by long periods (minutes) of silence, unlike in control cultures in which activity was more regular (figure 1*a*,*b*). As a result, the mean firing frequency of neurons was reduced on DIV 16–20 and there was no prominent peak in mean firing rate on DIV 20, as observed in the control groups (figure 1*d*). Detailed analysis of bursts revealed that the

frequency of burst of bursts generation in the group treated with the active heparinase was much higher from DIV 16 compared with the groups treated with PBS or heat-inactivated heparinase (figure 1*e*). Heparinase-induced bursting activity peaked at DIV 20 (figure 1*e*), which corresponded to the day with maximum frequency of spike generation in the control groups.

(b) Up-scaling of excitatory synaptic currents by heparinase treatment

We next considered whether the changes in network excitability induced by enzymatic removal of HSHSs were related to alterations of the excitation/inhibition ratio. To this aim, we performed concomitant recordings of miniature excitatory and inhibitory postsynaptic currents (mEPSCs and mIPSCs, respectively) after heparinase treatment performed as described in the previous section. Removal of HSHSs selectively increased excitatory synaptic input on DIV 18, while leaving unaffected spontaneous inhibitory synaptic transmission (figure 2*a*,*b*), with a consequent increase in excitation/inhibition ratio. Specifically, mEPSC amplitude and frequency were augmented by 64 and 160%, respectively; no changes in mEPSC waveform were observed (electronic supplementary material, figure S2). These findings suggest that HSPGs play a major role in shaping excitatory synaptic transmission during maturation of neural networks.

Considering that ECM regulates several aspects of homeostatic synaptic plasticity (HSP) [9–11], we next asked whether the regulation of excitatory synaptic transmission by HSPGs shared some mechanisms with HSP. Indeed, we noted that heparinase-dependent up-scaling of mEPSC amplitudes followed a multiplicative rule (figure 2*c*), as seen for synaptic scaling in response to activity deprivation in primary neuronal cultures [8,12].

(c) Biochemical modifications after heparinase treatment

The observed increase in mEPSC amplitude and frequency could be the consequence of elevated expression of AMPAR subunits. Therefore, we next investigated whether the levels of GluA1 and GluA2, the two major AMPAR subunits at central synapses, were altered by chronic heparinase treatment. Western blot analysis of GluA1 and GluA2 expression was performed on primary hippocampal neurons on DIV 19 after heparinase treatment starting from DIV 11, as in electrophysiological experiments (figure 3*a*). Heparinase treatment resulted in a statistically significant 1.32 ± 0.03-fold increase in the protein levels for GluA1 relative to untreated controls ($n = 5$, $p < 0.001$), but not for GluA2 (1.15 ± 0.07-fold, $n = 3$, $p > 0.1$; figure 3*c*). This upregulation of GluA1 expression was detected already on DIV 14 and thus preceded appearance of epileptiform activity (electronic supplementary material, figure S3).

A previous study has shown that HSP-associated upregulation of GluA1 protein levels could be triggered by an increase in β Ca^{2+}/calmodulin-dependent protein kinase II (βCaMKII) expression [13]. Because regulation of kinase activity of both α and β CaMKII isoforms strongly depends on autophosphorylation at Thr286 and Thr287, respectively (reviewed in [14]), we decided to assess whether heparinase treatment affects protein expression or autophosphorylation of these two major forebrain CaMKII isoforms in primary hippocampal neurons (figure 3*b*). Indeed, we found that heparinase upregulated autophosphorylation of both α and β CaMKII by 3.06 ± 0.47-fold ($n = 3$, $p < 0.05$) and 2.26 ± 0.26-fold ($n = 4$, $p < 0.05$), respectively, without altering total protein levels (0.97 ± 0.05-fold, $n = 4$, $p > 0.1$ and 1.06 ± 0.06-fold, $n = 4$, $p > 0.1$, respectively; figure 3*c*).

Because CaMKII phosphorylates GluA1 on Ser831 and this site is critical for CaMKII-induced potentiation of GluA1 currents [15], we verified whether phosphorylation of GluA1 at this site is increased after heparinase treatment. Using phospho-specific antibodies, we observed a tendency in increase of P-Ser831 GluA1/total GluA1 ratio (1.21 ± 0.14, $p = 0.16$, $n = 4$; electronic supplementary material, figure S4A, B) and a significant increase in the level of P-Ser831 GluA1/tubulin ratio (1.60 ± 0.11, $p < 0.05$, $n = 4$; electronic supplementary material, figure S4A, C) in heparinase-treated cultured hippocampal neurons, as compared to control. Thus, we show that heparinase treatment elevates expression of both the total and Ser831-phosphorylated GluA1.

Taken together, these data suggest that HSHS removal upregulates GluA1 expression, possibly as a consequence of the increase in CaMKII autophosphorylation.

3. Discussion

At the network level, the heparinase treatment led to a reduction in mean firing rate, with the appearance of highly synchronous epileptiform discharges separated by long periods of inactivity. Generation of epileptiform activity in heparinase-treated cultures is noteworthy in the light of multiple autistic features of HS-deficient *Ext1* knockout mice [7] and frequent appearance of seizures as comorbidity in autism spectrum disorders [16].

At the synaptic level, we revealed that heparinase treatment elevated glutamatergic transmission in hippocampal neurons, while no changes in efficacy of inhibitory transmission were detected. We speculate that the resulting shift in excitation/inhibition ratio may be the cause of epileptiform activity in heparinase-treated cultures. Linear up-scaling of mEPSC amplitudes was accompanied by upregulation of GluA1 expression and upregulation of CaMKII signalling, as reported in previous studies on HSP [13,17], thus suggesting a mechanistic link between degradation of HSs and induction of HSP. Considering the autistic phenotype of *Ext1* mice deficient in HS, our data support an emerging link between HSP and autism spectrum disorders [18]. Interestingly, in *Ext1*-deficient mice, a reduction rather than elevation of excitatory transmission was observed in the amygdala [7]. This is, however, not surprising because (i) HSPGs are required for synaptogenesis [4,5] and (ii) in the nervous tissue/organotypic situation the pattern of synaptic changes underlying HSP is expected to be complex: synaptic upscaling may be induced in a subset of synapses while others can be downscaled [19]. From the present and previous [19] studies, it is plausible to reveal upscaling of mEPSCs in the CA1 and dentate gyrus principal cells after enzymatic removal of hippocampal HSHSs *in vivo* as well as in *Ext1*-deficient mice.

A parallel study published in this issue [20] demonstrates that induction of homeostatic plasticity in neuronal cell cultures by prolonged suppression of neuronal firing is accompanied by brevican proteolytic processing by ADAMTS4 at inhibitory as well as excitatory synapses. The authors suggested that such 'ECM remodelling in conditions of homeostatic plasticity may liberate synapses to allow for a higher degree of structural

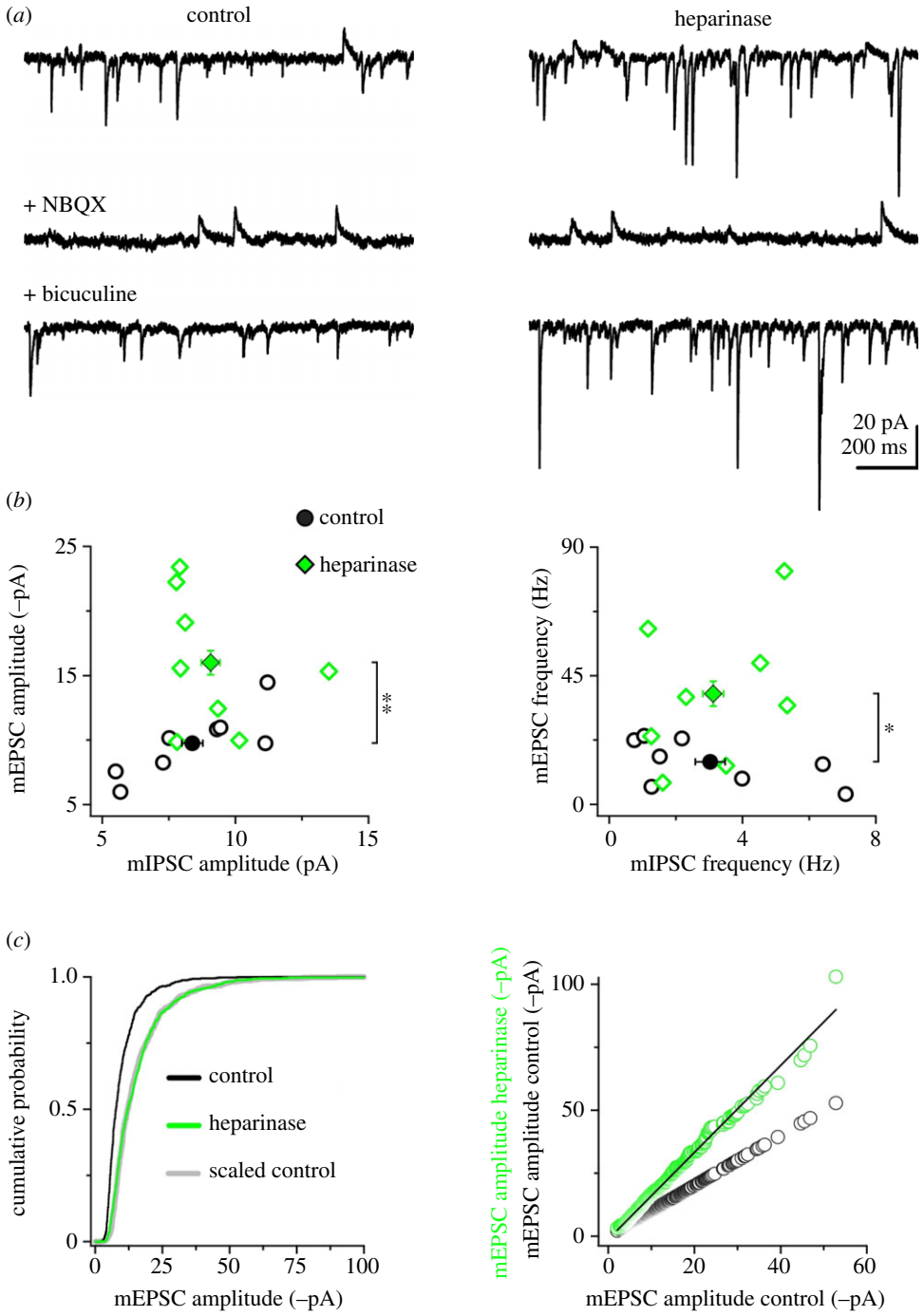

Figure 2. Chronic heparinase treatment increases mEPSC amplitude and frequency. (*a*) Simultaneous recordings of mEPSCs and mIPSCs from representative hippocampal neurons of control (left) and heparinase-treated cultures (right). Top, under basal conditions, mEPSCs and mIPSCs are detected as downward and upward going events, respectively. Middle, application of the AMPAR antagonist NBQX (1 μM) isolates mIPSCs. Bottom, wash-out of NBQX and application of the $GABA_A$ receptor antagonist bicuculline (10 μM) isolates mEPSCs (bottom). (*b*) Quantification of experiments as in (*a*) for mEPSC/mIPSC amplitude (left) and mEPSC/mIPSC frequency (right). Open symbols are averages for individual cells; filled symbols are average cell populations. Heparinase treatment increases mEPSC amplitude and frequency (**$p = 0.01$; *$p = 0.03$; unpaired two-tailed Student's *t*-test, $n = 8$ cells). (*c*) Left, cumulative distributions of mEPSC amplitude (first 100 events per cell) in control (black line) and heparinase-treated cultures (green line). The distribution of the scaled control data (grey line) overlapped with the distribution of heparinase-treated mEPSCs ($p = 0.536$ between heparinase and scaled control, $p < 0.0009$ between heparinase and control; Kolmogorov–Smirnov test), suggesting a global up-scaling of mEPSCs upon heparinase treatment. Right, mEPSCs (first 100 events per cell) were ranked according to their amplitudes and plotted against the ranked control distribution (open green circles: heparinase versus control; open black circles: control versus control). The black line represents the best linear fit ($f(x) = b \times x + a$, with $b = 1.7254 \pm 0.00439$ and $a = -1.2444 \pm 0.0511$) used to scale the control cumulative distribution in the left panel. (Online version in colour.)

plasticity', i.e. be an important permissive event. Our study provides a complementary view, highlighting that a deficit in glycans associated with ECM and membrane proteins may play a causal role in induction of HSP.

HSP can be induced *in vitro* by inhibition of all spiking activity with tetrodotoxin, or by inhibition of AMPARs with NBQX or by the inhibitor of L-type voltage-dependent Ca^{2+} channels (L-VDCCs) nifedipine [8,17], suggesting that the reduction in tonic Ca^{2+} influx mediated by these channels might be the key event in this form of plasticity [17]. Interestingly, heparin binds L-VDCC [21]; moreover, another polyanionic glycan, hyaluronic acid, supports activity of L-VDCCs [22] and its enzymatic removal

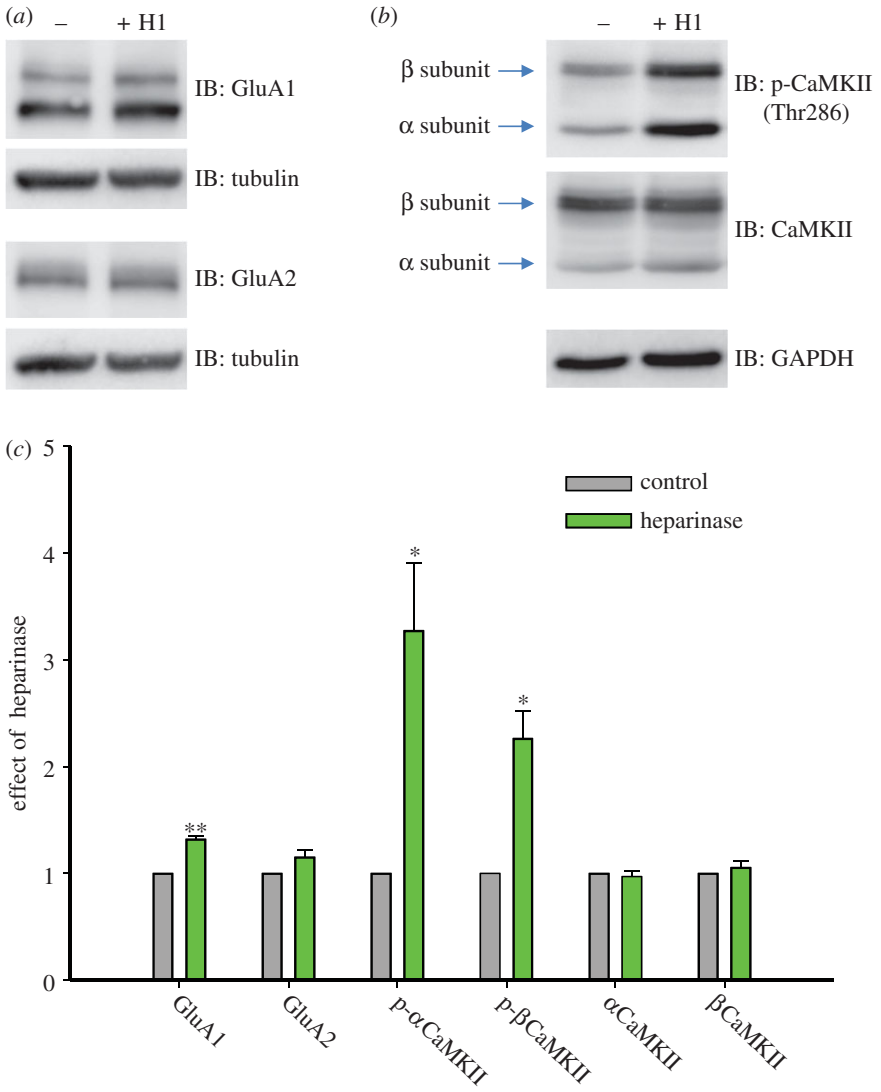

Figure 3. Heparinase upregulates GluA1 expression and CaMKII activity. Mouse hippocampal neurons were treated with vehicle or heparinase (H1) on DIV 11, 14 and 17. On DIV 19 cells were lysed and 30 mg of extracts were subjected to immunoblotting (IB). (*a*) Membranes were probed with anti-GluA1 or anti-GluA2 and anti-tubulin antibodies, to standardize the level of GluA subunit expression. (*b*) To assess autophosphorylation level of CaMKII α and β isoforms, membranes were first incubated with anti-phospho-Thr286 CaMKII antibody and after stripping with an anti-CaMKII antibody (to estimate the total CaMKII level). The lower part of the membrane was probed with anti-GAPDH to standardize the level of protein expression. (*c*) Bar graphs representing statistical evaluation of experiments as in (*a*) and (*b*). Data are shown as mean + s.e.m. There is a statistically significant increase in GluA1 expression level (**$p < 0.001$; $n = 5$) and in α (*$p < 0.05$; $n = 3$) and in β (*$p < 0.05$; $n = 4$) CaMKII autophosphorylation upon heparinase treatment (the values are normalized relative to the control for each Western blot; Paired *t*-test or Signed Rank Test was used for statistical evaluation). (Online version in colour.)

leads to appearance of epileptiform activity similar to that reported in this study [23]. Thus, modulation of L-VDCC activity can be one of the mechanisms by which a deficit of HSs induces HSP. Another option would be HS-mediated modulation of β3 integrins, which are other key players in HSP [12]. This option is also plausible because HSs bind to α5β1 and αvβ3 integrins and integrin ligands may have the same binding site to interact with either integrins or HSs [24], and hence removal of HSs may shift interaction of such ligands towards integrins. Further experiments are warranted to verify these possible mechanisms and to investigate seizure generation/up-scaling of mEPSCs after *in vivo* application of heparinase I or in *Ext1*-deficient mice.

4. Material and methods

(a) Reagents

The following primary antibodies were used in the study: rabbit polyclonal anti-GluA1 and -GluA2 (AGC-004 and AGC-005, respectively; Alomone Labs), rabbit polyclonal anti-GluA1 phospho-Ser831 (AB5847, Millipore), rabbit polyclonal anti-CaMKII (RU16, previously described to recognize both α and β isoforms [25]), rabbit polyclonal anti-phospho-Thr286 CaMKII (p1005–286, PhosphoSolutions), mouse monoclonal anti-β-tubulin (T5201; Sigma), mouse monoclonal anti-glyceraldehyde-3-phosphate dehydrogenase (GAPDH) (MAB374, clone 6C5; Millipore), mouse anti-GFAP (Sigma, G3893) and rabbit anti-MAP2 (Synaptic Systems, 188002). The following secondary antibodies were used: horseradish peroxidase (HRP)-conjugated goat anti-mouse (PR31430) and goat anti-rabbit antibodies (PR31460) from Termo Scientific, highly cross-adsorbed Alexa Fluor 488 goat anti-mouse IgG (A11029) and Alexa Fluor 568 goat anti-mouse igG (A111036) from Invitrogen.

ECL prime Western blotting detection reagent (RPN2232) was from GE Healthcare. Page ruler prestained protein ladder plus (PR26620) and non-fat dried milk powder (EMR180001) Westran CS and 0.45 µm polyvinylidene fluoride (PVDF) blotting membrane (10485289) were purchased from Euroclone. Phosphatase inhibitor cocktail 2 for tyrosine protein phosphatases, acid and alkaline (P5726) and phosphatase inhibitor

cocktail 3 for serine/threonine protein phosphatases and L-isozymes of alkaline phosphatase (P0044), aprotinin from bovine lung (A1153), pefabloc (76307) and leupeptin were from Sigma, BCA Assay Kit (PR23225) was from Termo Scientific.

Heparinase I from *Flavobacterium heparinum* (EC 4.2.2.7, Sigma-H2519) was dissolved in phosphate-buffered saline (PBS) to 200× (100 U ml^{-1}) stock and aliquots were kept at −80°C before use.

(b) Culturing and treatment of neural cells on microelectrode arrays

Hippocampal cells were dissociated from embryonic mice (on embryonic day 18) and plated with a high initial density of approximately 3000 cells mm^{-2} on 6-well microelectrode arrays (MEAs; Multi Channel Systems MCS GmbH, Germany) pre-treated with polyethyleneimine (Sigma P3143) and laminin (Sigma L2020). C57BL6J mice were killed by cervical vertebra dislocation. Embryos were removed and decapitated. The entire hippocampi were dissected under sterile conditions. Hippocampi were cut in Ca^{2+}- and Mg^{2+}- free PBS (PBS-minus). After enzymatic digestion for 20 min by 0.25% trypsin-EDTA (Invitrogen 25200–056) at 37°C, cells were separated by trituration (20 passes) in PBS using a 1 ml pipette tip. After being passed, the solution was centrifuged at 1500*g* for 2 min, and the cell pellet was immediately re-suspended in Neurobasal medium (Invitrogen 21103-049) with 2% B27 (Invitrogen 17504-044), 0.5 mM L-glutamine (Invitrogen 25030-024), 5% fetal calf serum (PanEco K055) and 0.05% gentamycin (Sigma G1272) (NBM1). The dissociated cells were plated in a 20 µl droplet covering the centre of the culture dish on a 1 mm^2 electrode region of each part of a 6-well MEA, forming a dense monolayer [26]. After 2 h, the dishes were filled with 0.5 ml of NBM1. After 3 days, one half of the plating medium was replaced by a medium containing Neurobasal medium with 2% B27, 1 mM L-glutamine and 0.05% gentamycin (NBM2). Glial growth was not suppressed. One half of the medium was changed every 3 days. The cells were cultured under constant conditions of 37°C, 5% CO_2 and 95% air at saturating humidity in a cell culture incubator (MCO-18AIC, Sanyo).

One group of cultures received heparinase I treatment (0.5 U ml^{-1}), the second group received the same volume of PBS (vehicle control group) and the third group was treated with heat-inactivated heparinase I (100°C for 30 min). The heparinase was added to the cell cultures starting from 11th DIV every third day during the changes of culture medium. This heparinase I concentration used was reported to provide the effect close to maximal [27].

(c) Immunoblot analysis

To access the expression level of endogenous proteins and the level of their phosphorylation, 30 µg of extracts from hippocampal cells (250 000–300 000 plated cells per well, treated in the same way as for microelectrode array recordings) were resuspended in reducing electrophoresis sample buffer 2× (SB2×: 4% SDS, 20% glycerol, 120 mM TRIS, 0.01% bromophenol blue, pH 7.8, 0.2 M DTT, 4% β-mercaptoethanol). Protein extracts were separated by SDS-PAGE on 7 and 9% acrylamide gels, transferred to the PVDF membranes with 0.45 µm pore size and after having been blocked for 40–90 min at room temperature with 5% milk in TBS-T buffer probed with appropriate primary antibody at 4°C overnight and subsequently with HRP-goat anti-mouse or goat anti-rabbit secondary antibodies for 1–2 h at room temperature. Proteins were captured by chemiluminescent detection using ImageQuant LAS 4000 (GE Healthcare, 28-9558-10). Densitometric analysis of the digital images was performed using ImageJ software. To assess the autophosphorylation level of α and β CaMKII, cell membranes were first incubated with anti-phospho-Thr286 CaMKII and after being stripped were reprobed with anti-CaMKII to analyse the total level of protein. The ratios of autophosphorylation signal to total amount of CaMKII protein were calculated. To estimate expression level of GluA1, GluA2, and α and β isoforms of CaMKII, the amount of protein present in each sample was standardized to the level of tubulin or GAPDH. To evaluate GluA1 phosphorylation on Ser831, the ratios between phospho-Ser831 signal to (i) total amount of GluA1 protein or (ii) tubulin expression were calculated.

For statistical evaluation and the graphical representation of the data, the SigmaPlot v. 12.5 software was used. The average ±s.e.m. (standard error) was calculated from three or more experiments for the experimental (heparinase-treated) group, normalized to the control (untreated) group. Statistical evaluation was carried out by paired *t*-test or Signed Rank Test.

(d) Patch clamp recordings

Either heparinase I (0.5 U ml^{-1}) or vehicle was applied to mouse primary hippocampal cultures every third day starting at DIV 11. Whole-cell patch clamp recordings were performed at room temperature from hippocampal pyramidal neurons at DIV 18. Cultures were continuously perfused with an aCSF containing: 130 mM NaCl, 2.5 mM KCl, 0.5 mM $CaCl_2$, 10 mM $MgCl_2$, 10 mM D-glucose and 10 mM HEPES-NaOH (pH 7.38; osmolarity adjusted to 290 mOsm). Blockers of sodium channels (0.5 µM tetrodotoxin), NMDARs (50 µM D-APV) and L-VDCCs (10 µM nimodipine) were routinely included in the aCSFs. The intracellular solution contained: 150 mM K-gluconate, 3 mM KCl, 0.5 mM EGTA, 4 mM Mg-ATP, 0.5 mM Na_3-GTP, 20 mM K_2-creatine phosphate and 10 mM HEPES-KOH (pH 7.28; osmolarity adjusted to 280 mOsm). In these conditions, the estimated reversal potential for Cl^- was about −100 mV. Recordings were performed with an EPC10 amplifier (HEKA Elektronik, Germany). Pipette resistance was 2.5–3 MΩ and there were no significant differences between compared groups in series resistances and holding currents.

Miniature excitatory and inhibitory postsynaptic currents (mEPSCs and mIPSCs) were recorded simultaneously at a holding potential of −50 mV as inward and outward currents, respectively. After 2 min, mIPSCs and mEPSCs were sequentially isolated by applying NBQX (1 µM; 5 min) and subsequently bicuculline (10 µM; 15 min). Recordings were filtered at 5 kHz and digitized at 50 kHz. mIPSCs and mEPSCs were scored over the last minute of NBQX and bicuculline applications, respectively; detection was performed off-line in ClampFit (Axon Instruments, USA) using the threshold search algorithm; detection level was set 2 times higher than the baseline noise and raw data were visually inspected to eliminate false events; cells with noisy or unstable baselines were discarded. The mEPSC and mIPSC weighted decay time constant was calculated for each single event in Igor Pro 6.03 (Wavemetrics Inc., USA) as described elsewhere [12].

Input resistance (R_{in}), membrane capacitance (C_m) and resting potential (V_m) were not significantly different in the two groups (R_{in} was 403 ± 32 MΩ for control and 287 ± 27 MΩ for heparinase, $p = 0.10$; C_m was 140 ± 12 pF for control and 130 ± 9 pF for heparinase, $p = 0.74$; V_m was −49.5 ± 0.7 mV for control and −50.3 ± 0.8 mV for heparinase, $p = 0.48$; $n = 8$ cells each, unpaired two-tailed Student's *t*-test).

(e) Microelectrode array recordings

Extracellular potentials were acquired simultaneously through a MEA120 system (Multi Channel Systems MCS GmbH, Germany), composed by two amplifiers allowing simultaneous recordings from two 60-channel planar indium tin-oxide (ITO) electrode arrays. Each chamber of the 6-well MEAs adopted for this study was composed of 3 × 3 (nine) electrodes with a 30 µm diameter

and a 200 µm interelectrode spacing plus one reference electrode. Data were recorded at 10 kHz per channel sampling rate. To analyse the neural network activity, we recorded spontaneous bursting activity for 15 min. All of the signal analyses and statistics were performed using custom made software SPYCODE (Matlab) [28]. The detection of recorded extracellular spikes was based on the Precise Timing Spike Detection method [29]. The detection of bursts was based on the detection of peaks in the inter-spike interval histogram. To detect bursts of bursts in the spiking activity, we applied the threshold detection algorithm, in which the threshold was estimated using the inter-burst interval histogram as the value corresponding to the minimum between the peak for regular bursts and the next peak [30].

All data are presented as the mean ± s.e.m. Statistical analysis was performed using a two-way analysis of variance (ANOVA) implemented in the SIGMAPLOT 11.0 program (Systat Software Inc.). Student–Newman–Keuls (SNK) was used as a post hoc ANOVA test. The difference between groups was considered significant if the p-value was less than 0.05.

Acknowledgements. We thank Marina Nanni and Claudia Chiabrera for excellent technical assistance.

Funding statement. This study was supported by Italian Institute of Technology (IIT), German Center for Neurodegenerative Diseases (DZNE), the Russian Federation governmental grant no. 11.G34.31. 0012, Neuron EraNet TargetECM, and by COST Action BM1001 'Brain Extracellular Matrix in Health and Disease'.

References

1. Maeda N, Ishii M, Nishimura K, Kamimura K. 2011 Functions of chondroitin sulfate and heparan sulfate in the developing brain. *Neurochem. Res.* **36**, 1228–1240. (doi:10.1007/s11064-010-0324-y)
2. Kirn-Safran C, Farach-Carson MC, Carson DD. 2009 Multifunctionality of extracellular and cell surface heparan sulfate proteoglycans. *Cell Mol. Life Sci.* **66**, 3421–3434. (doi:10.1007/s00018-009-0096-1)
3. Fico A, Maina F, Dono R. 2011 Fine-tuning of cell signaling by glypicans. *Cell Mol. Life Sci.* **68**, 923–929. (doi:10.1007/s00018-007-7471-6)
4. Dityatev A, Dityateva G, Sytnyk V, Delling M, Toni N, Nikonenko I, Muller D, Schachner M. 2004 Polysialylated neural cell adhesion molecule promotes remodeling and formation of hippocampal synapses. *J. Neurosci.* **24**, 9372–9382. (doi:10.1523/JNEUROSCI.1702-04.2004)
5. Allen NJ, Bennett ML, Foo LC, Wang GX, Chakraborty C, Smith SJ, Barres BA. 2012 Astrocyte glypicans 4 and 6 promote formation of excitatory synapses via GluA1 AMPA receptors. *Nature* **486**, 410–414. (doi:10.1038/nature11059)
6. Lauri SE, Kaukinen S, Kinnunen T, Ylinen A, Imai S, Kaila K, Taira T, Rauvala H. 1999 Regulatory role and molecular interactions of a cell-surface heparan sulfate proteoglycan (N-syndecan) in hippocampal long-term potentiation. *J. Neurosci.* **19**, 1226–1235.
7. Irie F, Badie-Mahdavi H, Yamaguchi Y. 2012 Autism-like socio-communicative deficits and stereotypies in mice lacking heparan sulfate. *Proc. Natl Acad. Sci. USA* **109**, 5052–5056. (doi:10.1073/pnas.1117881109)
8. Turrigiano GG, Leslie KR, Desai NS, Rutherford LC, Nelson SB. 1998 Activity-dependent scaling of quantal amplitude in neocortical neurons. *Nature* **391**, 892–896. (doi:10.1038/36103)
9. Dityatev A, Schachner M, Sonderegger P. 2010 The dual role of the extracellular matrix in synaptic plasticity and homeostasis. *Nat. Rev. Neurosci.* **11**, 735–746. (doi:10.1038/nrn2898)
10. Gundelfinger ED, Frischknecht R, Choquet D, Heine M. 2010 Converting juvenile into adult plasticity: a role for the brain's extracellular matrix. *Eur. J. Neurosci.* **31**, 2156–2165. (doi:10.1111/j.1460-9568.2010.07253.x)
11. Thalhammer A, Cingolani LA. 2014 Cell adhesion and homeostatic synaptic plasticity. *Neuropharmacology* **78**, 23–30. (doi:10.1016/j.neuropharm.2013.03.015)
12. Cingolani LA, Goda Y. 2008 Differential involvement of beta3 integrin in pre- and postsynaptic forms of adaptation to chronic activity deprivation. *Neuron Glia Biol.* **4**, 179–187. (doi:10.1017/S1740925X 0999024X)
13. Groth RD, Lindskog M, Thiagarajan TC, Li L, Tsien RW. 2011 Beta Ca^{2+}/CaM-dependent kinase type II triggers upregulation of GluA1 to coordinate adaptation to synaptic inactivity in hippocampal neurons. *Proc. Natl Acad. Sci. USA* **108**, 828–833. (doi:10.1073/pnas.1018022108).
14. Coultrap SJ, Bayer KU. 2012 CaMKII regulation in information processing and storage. *Trends Neurosci.* **35**, 607–618. (doi:10.1016/j.tins.2012.05.003)
15. Barria A, Derkach V, Soderling T. 1997 Identification of the Ca^{2+}/calmodulin-dependent protein kinase II regulatory phosphorylation site in the alpha-amino-3-hydroxyl-5-methyl-4-isoxazole-propionate-type glutamate receptor. *J. Biol. Chem.* **272**, 32 727–32 730. (doi:10.1074/jbc.272.52.32727)
16. Levisohn PM. 2007 The autism-epilepsy connection. *Epilepsia* **48**(Suppl. 9), 33–35. (doi:10.1111/j.1528-1167.2007.01399.x)
17. Thiagarajan TC, Lindskog M, Tsien RW. 2005 Adaptation to synaptic inactivity in hippocampal neurons. *Neuron* **47**, 725–737. (doi:10.1016/j.neuron.2005.06.037)
18. Wondolowski J, Dickman D. 2013 Emerging links between homeostatic synaptic plasticity and neurological disease. *Front Cell Neurosci.* **7**, 223. (doi:10.3389/fncel.2013.00223)
19. Kim J, Tsien RW. 2008 Synapse-specific adaptations to inactivity in hippocampal circuits achieve homeostatic gain control while dampening network reverberation. *Neuron* **58**, 925–937. (doi:10.1016/j.neuron.2008.05.009)
20. Valenzuela JC, Heise C, Franken G, Singh J, Schweitzer B, Seidenbecher CI, Frischknecht R. 2014 Hyaluronan-based extracellular matrix under conditions of homeostatic plasticity. *Phil. Trans. R. Soc. B* **369**, 20130606. (doi:10.1098/rstb.2013.0606)
21. Knaus HG, Scheffauer F, Romanin C, Schindler HG, Glossmann H. 1990 Heparin binds with high affinity to voltage-dependent L-type Ca^{2+} channels. Evidence for an agonistic action. *J. Biol. Chem.* **265**, 11 156–11 166.
22. Kochlamazashvili G *et al*. 2010 The extracellular matrix molecule hyaluronic acid regulates hippocampal synaptic plasticity by modulating postsynaptic L-type Ca^{2+} channels. *Neuron* **67**, 116–128. (doi:10.1016/j.neuron.2010.05.030)
23. Vedunova M, Sakharnova T, Mitroshina E, Perminova M, Pimashkin A, Zakharov Y, Dityatev A, Mukhina I. 2013 Seizure-like activity in hyaluronidase-treated dissociated hippocampal cultures. *Front. Cell Neurosci.* **7**, 149. (doi:10.3389/fncel.2013.00149)
24. Faye C, Moreau C, Chautard E, Jetne R, Fukai N, Ruggiero F, Humphries MJ, Olsen BR, Ricard-Blum S. 2009 Molecular interplay between endostatin, integrins, and heparan sulfate. *J. Biol. Chem.* **284**, 22 029–22 040. (doi:10.1074/jbc.M109.002840)
25. Menegon A, Verderio C, Leoni C, Benfenati F, Czernik AJ, Greengard P, Matteoli M, Valtorta F. 2002 Spatial and temporal regulation of Ca^{2+}/calmodulin-dependent protein kinase II activity in developing neurons. *J. Neurosci.* **22**, 7016–7026.
26. Potter SM, DeMarse TB. 2001 A new approach to neural cell culture for long-term studies. *J. Neurosci. Methods* **110**, 17–24. (doi:10.1016/S0165-0270(01)00412-5)
27. Jiang J, Wu X, Tang H, Luo G. 2013 Apolipoprotein E mediates attachment of clinical hepatitis C virus to hepatocytes by binding to cell surface heparan sulfate proteoglycan receptors. *PLoS ONE* **8**, e67982. (doi:10.1371/journal.pone.0067982)
28. Bologna LL, Pasquale V, Garofalo M, Gandolfo M, Baljon PL, Maccione A, Martinoia S, Chiappalone M. 2010 Investigating neuronal activity by SPYCODE multi-channel data analyzer. *Neural Netw.* **23**, 685–697. (doi:10.1016/j.neunet.2010.05.002)
29. Maccione A, Gandolfo M, Massobrio P, Novellino A, Martinoia S, Chiappalone M. 2009 A novel algorithm for precise identification of spikes in extracellularly recorded neuronal signals. *J. Neurosci. Methods* **177**, 241–249. (doi:10.1016/j.jneumeth.2008.09.026)
30. Pasquale V, Martinoia S, Chiappalone M. 2010 A self-adapting approach for the detection of bursts and network bursts in neuronal cultures. *J. Comput. Neurosci.* **29**, 213–229. (doi:10.1007/s10827-009-0175-1)